Article

Charged Polypeptide Vesicles with Controllable Diameter

Eric P. Holowka, Darrin J. Pochan, and Timothy J. Deming

J. Am. Chem. Soc., **2005**, 127 (35), 12423-12428• DOI: 10.1021/ja053557t • Publication Date (Web): 16 August 2005

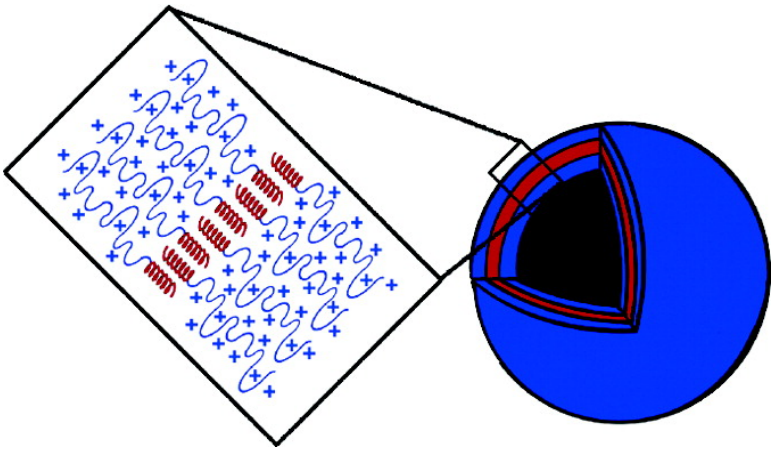

J|A|C|S
ARTICLES
Published on Web 08/16/2005

Charged Polypeptide Vesicles with Controllable Diameter

Eric P. Holowka,[†] Darrin J. Pochan,[‡] and Timothy J. Deming*[,§]

Contribution from the Materials Department, University of California at Santa Barbara, Santa Barbara, California 93106, Department of Materials Science and Engineering and Delaware Biotechnology Institute, University of Delaware, Newark, Delaware 19716, and Bioengineering Department, University of California at Los Angeles, California 90049

Received May 31, 2005; E-mail: demingt@seas.ucla.edu

Abstract: We report the preparation and characterization of charged, amphiphilic block copolypeptides that form stable vesicles and micelles in aqueous solution. Specifically, we prepared and studied the aqueous self-assembly of a series of poly(L-lysine)-*b*-poly(L-leucine) block copolypeptides, K_xL_y, where *x* ranged from 20 to 80 and *y* ranged from 10 to 30 residues, as well as the poly(L-glutamatic acid)-*b*-poly(L-leucine) block copolypeptide, $E_{60}L_{20}$. Furthermore, the vesicular assemblies show dynamic properties, indicating a high degree of membrane fluidity. This characteristic provides stimuli-responsive properties to the vesicles and allows fine adjustment of vesicle size using liposome-based extrusion techniques. Vesicle extrusion also provides a straightforward means to trap solutes, making the vesicles promising biomimetic encapsulants.

Introduction

There has been an abundance of research in recent years on the preparation and characterization of polypeptide based materials.[1] Since these polymers employ the building blocks of proteins, they begin to allow incorporation of the structures and functions of proteins into synthetic materials. These features are particularly desirable for control over nanoscale ordering via self-assembly,[2] coupling of synthetic materials to biological molecules as in sensors,[3] and the development of materials with increased capability to respond to living systems for tissue engineering and therapeutic delivery.[4] The structural feature common to most synthetic polypeptide materials is an amphiphilic block copolymer sequence, where either one or more polymer domains is peptidic and which is designed to self-assemble in aqueous solution.[5] Furthermore, the presence of an ordered chain conformation in the polypeptide domain typically strongly affects the nature of self-assembly.[1] Here, we report the preparation and characterization of charged, amphiphilic block copolypeptides that form stable vesicles and micelles in aqueous solution (Figure 1). Furthermore, the vesicular assemblies show dynamic properties, indicating a high degree of membrane fluidity. This characteristic provides stimuli-responsive properties to the vesicles and allows fine adjustment of vesicle size using liposome-based extrusion techniques. Vesicle extrusion also provides a straightforward means to trap solutes, making the vesicles promising biomimetic encapsulants.

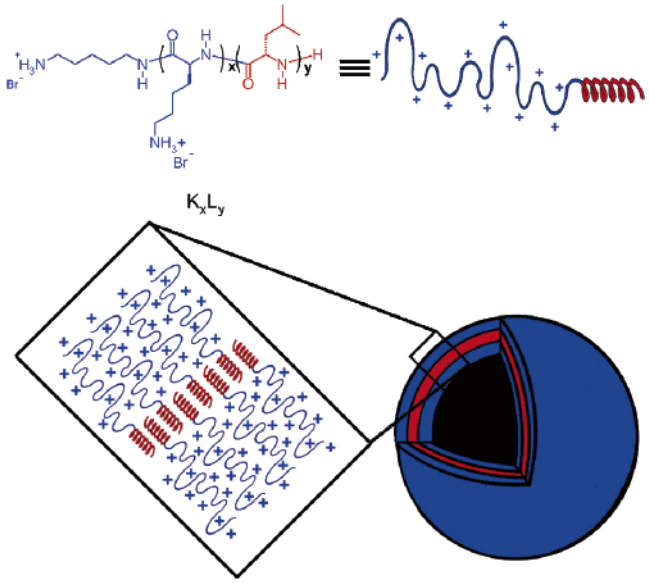

Figure 1. Schematic drawing showing proposed self-assembly of $K_{60}L_{20}$ into vesicles.

There are a few reports of polymer vesicles from charged, amphiphilic diblock copolymers. The poly(styrene)-*b*-poly(acrylic acid) system of Eisenberg is perhaps the best studied.[6]

[†] University of California at Santa Barbara.
[‡] University of Delaware.
[§] University of California at Los Angeles.

(1) (a) Vandermeulen, G. W. M.; Klok, H. A. *Macromol. Biosci.* **2004**, *4*, 383−398. (b) Klok, H. A. *Angew. Chem., Int. Ed.* **2002**, *41*, 1509−1513. (c) Deming, T. J. *Adv. Drug Delivery Rev.* **2002**, *54*, 1145−1155.
(2) (a) Cha, J. N.; Stucky, G. D.; Morse, D. E.; Deming, T. J. *Nature* **2000**, *403*, 289−292. (b) Belcher, A. M.; Wu, X. H.; Christensen, R. J.; Hansma, P. K.; Stucky, G. D.; Morse, D. E. *Nature* **1996**, *381*, 56−58.
(3) (a) Link, A. J.; Mock M. L.; Tirrell, D. A. *Curr. Opin. Biotechnol.* **2003**, *14*, 603−609. (b) Mao, C. B.; Solis, D. J.; Reiss, B. D.; Kottmann, S. T.; Sweeney, R. Y.; Hayhurst, A.; Georgiou, G.; Iverson, B.; Belcher, A. M. *Science* **2004**, *303*, 213−217.
(4) (a) Zhang, S.; Marini, D. N.; Hwang, W.; Santoso, S. *Curr. Opin. Chem. Biol.* **2002**, *6*, 865−871. (b) Silva, G. A.; Czeisler, C.; Niece, K. L.; Beniash, E.; Harrington, D. A.; Kessler, J. A.; Stupp, S. I. *Science* **2004**, *303*, 1352−1355.
(5) Schlaad, H.; Antonetti, M. *Eur. Phys. J. E* **2003**, *10*, 17−23.
(6) (a) Yu, K.; Eisenberg, A. *Macromolecules* **1998**, *31*, 3509−3518. (b) Luo, L.; Eisenberg, A. *Langmuir* **2001**, *17*, 6804−6811.

Table 1. Properties of 1 % (w/v) Suspensions of K_mL_n and E_mL_n Block Copolypeptides

copolypeptide	observed structure[a]	size[b]	CMC[c] (M)	found composition[d]	M_w/M_n[d]	PDI[e]
$K_{20}L_{20}$	S	30 μm		$K_{22}L_{17}$	1.29	
$K_{40}L_{20}$	F	15 μm		$K_{38}L_{18}$	1.11	
$K_{60}L_{20}$	V	960 nm	6.7×10^{-7}	$K_{61}L_{21}$	1.13	0.24
$K_{80}L_{20}$	A	50 μm	4.2×10^{-5}	$K_{78}L_{20}$	1.12	1.56
$K_{60}L_{10}$	M	25 nm	9.7×10^{-5}	$K_{61}L_7$	1.29	0.23
$K_{60}L_{30}$	V, A	5−10 μm	6.5×10^{-11}	$K_{61}L_{32}$	1.18	0.58
(*rac*-K)$_{60}$-L-L$_{10}$	M, A	175 nm	1.5×10^{-5}	*rac*-K_{62}-L−L_{12}	1.14	0.25
(*rac*-K)$_{60}$-L-L$_{20}$	V, A	1040 nm	5.0×10^{-6}	*rac*-K_{62}-L−L_{24}	1.18	0.38
(*rac*-K)$_{60}$-L-L$_{30}$	V, A	15 μm	4.1×10^{-8}	*rac*-K_{62}-L−L_{36}	1.12	0.62
L-K_{60}-(*rac*-L)$_{20}$	A	10 μm	3.7×10^{-6}	K_{61}-*rac*-L_{21}	1.23	1.65
(*rac*-K)$_{60}$-(*rac*-L)$_{20}$	A	10 μm	2.6×10^{-5}	rac-K_{65}-*rac*-L_{24}	1.34	1.75
$E_{60}L_{20}$	V	1210 nm	3.5×10^{-6}	$E_{62}L_{23}$	1.29	0.28

[a] Structure determined visually from DIC images and from DLS measurements (V = vesicle, A = irregular aggregate, S = membrane sheet, F = fiber, M = micelle). [b] Average assembly size as determined visually from DIC images for aggregates greater than 1 μm. For assemblies 1 μm and smaller, average size was determined by DLS measurements at 90° on samples that were extruded through 1 μm PC membranes. [c] Critical micelle concentrations (CMC) were determined using pyrene fluorescence at 20 °C. [d] Found compositions and M_w/M_n were determined using gel permeation chromatography/light scattering (GPC/LS). [e] Assembly polydispersities (PDI) were determined using DLS.

These vesicles are assembled in organic solvents, but the resulting frozen assemblies in water can be prepared with a range of diameters. Nolte's group has also reported the formation of charged vesicles, in mixture with other assemblies, using poly(styrene)-*b*-poly(isocyanide) copolymers.[7] The groups of Lecommandoux[8] and Schlaad[9] independently reported vesicle formation using poly(butadiene)-*b*-poly(L-glutamate) copolymers, where the degree of ionization of the polypeptide segment and ionic strength were found to vary vesicle diameter from ca. 100 to 150 nm. Recently, Lecommandoux's group also reported vesicle formation from the entirely peptide-based copolymer poly(L-lysine)-*b*-poly(L-glutamate), which self-assembles under both acidic (pH < 4) and basic (pH > 10) conditions.[10] Previously, we reported the preparation of amphiphilic diblock copolypeptide systems that form vesicular membranes in water,[11] as well as those that form hydrogel networks.[12] The key difference between these two systems was the presence of highly charged polypeptide segments in the hydrogels (e.g., poly(L-lysine)), which acted to distort the flat membranes found with the vesicle-forming uncharged copolypeptides into twisted fibrillar networks.[13] We reasoned that use of shortened charged segments would relax repulsive polyelectrolyte interactions and allow formation of charged polypeptide membranes. Consequently, we prepared and studied the aqueous self-assembly of a series of poly(L-lysine)-*b*-poly(L-leucine) block copolypeptides, K_xL_y, where *x* ranged from 20 to 80 and *y* ranged from 10 to 30 residues.

Results and Discussion

The K_xL_y diblock copolypeptide amphiphiles (Table 1) were synthesized using transition metal-mediated α-amino acid *N*-carboxyanhydride polymerizations, which allow control over polypeptide chain length and composition.[14] The poly(L-lysine·HBr) segments are highly charged polyelectrolytes at neutral pH and dissolve readily in water.[15] The hydrophobic poly(L-leucine) domains, when sufficiently large, can adopt regular α-helical conformations that aggregate and are insoluble in water.[16] In earlier work, we found that samples with high K to L molar ratios (e.g., $K_{180}L_{20}$) could be dissolved directly into deionized (DI) water, yielding transparent hydrogels.[12,13] For the samples of this study, containing lower K to L ratios, it was found that addition of lyophilized copolymer to DI water yielded only suspensions of ill-defined aggregates. We reasoned that, similar to the polymeric amphiphiles prepared by Eisenberg, well ordered assemblies could be obtained if copolymer assembly was annealed using organic cosolvents to impart fluidity to kinetically frozen aggregates.[6] Helical poly(L-leucine) is known to be highly intractable, dissolving only in strongly H-bonding solvents such as TFA and only swelling in polar organic solvents such as THF and DMF.[16] After experimentation with many water miscible organic solvents (including TFA, THF, MeOH, EtOH) we found that use of THF−H_2O mixtures gave highly reproducible and regular copolypeptide assemblies. For all the samples in this study, lyophilized copolymer was first swelled in THF and dispersed using a sonication bath, followed by addition of an equal volume of deionized water, which yielded slightly turbid suspensions. Dynamic light scattering (DLS) analysis of these suspensions gave highly variable results, with apparent assembly diameters ranging from 200 nm to 8 μm. These suspensions were then exhaustively dialyzed against DI water to remove the THF and give the annealed polypeptide assemblies at concentrations of ca. 1.0 wt %.

In our first series of copolymers, the size of the oligoleucine domain was held constant at 20 residues, and the oligolysine domain was varied from 20 to 80 residues in length (Table 1, Figure 2). The $K_{20}L_{20}$ and $K_{40}L_{20}$ samples became highly turbid after dialysis. Analysis of these assemblies using differential interference contrast optical microscopy (DIC) revealed the presence of large, sheetlike membranes for $K_{20}L_{20}$ and thin fibrils for $K_{40}L_{20}$ (Figure 2). The $K_{60}L_{20}$ sample was most promising, as only large vesicular assemblies (ca. 1−3 μm

(7) Cornelissen, J. J. L. M.; Fischer, M.; Sommerdijk, N. A. J. M.; Nolte, R. J. M. *Science* **1998**, *280*, 1427−1430.
(8) Chécot, F.; Lecommandoux, S.; Gnanou, Y.; Klok, H.-A. *Angew. Chem., Int. Ed.* **2002**, *41*, 1340−1343.
(9) Kukula, H.; Schlaad, H.; Antonietti, M.; Förster, S. *J. Am. Chem. Soc.* **2001**, *124*, 1658−1663.
(10) Rodriguez-Hernández, J.; Lecommandoux, S. *J. Am. Chem. Soc.* **2005**, *127*, 2026−2027.
(11) Bellomo, E.; Wyrsta, M. D.; Pakstis, L.; Pochan, D. J.; Deming, T. J. *Nat. Mater.* **2004**, *3*, 244−248.
(12) Nowak, A. P.; Breedveld, V.; Pakstis, L.; Ozbas, B.; Pine, D. J.; Pochan, D.; Deming, T. J. *Nature* **2002**, *417*, 424−428.
(13) Breedveld, V.; Nowak, A. P.; Sato, J.; Deming, T. J.; Pine, D. J. *Macromolecules* **2004**, *37*, 3943−3953.
(14) (a) Deming, T. J. *Nature* **1997**, *390*, 386−389. (b) Deming, T. J. *J. Polym. Sci. Polym. Chem. Ed* **2000**, *38*, 3011−3018.
(15) Katchalski, E.; Sela, M. *Adv. Protein Chem.* **1958**, *13*, 243−492.
(16) Fasman, G. D. *Prediction of Protein Structure and the Principles of Protein Conformation*; Plenum: NY, 1989.

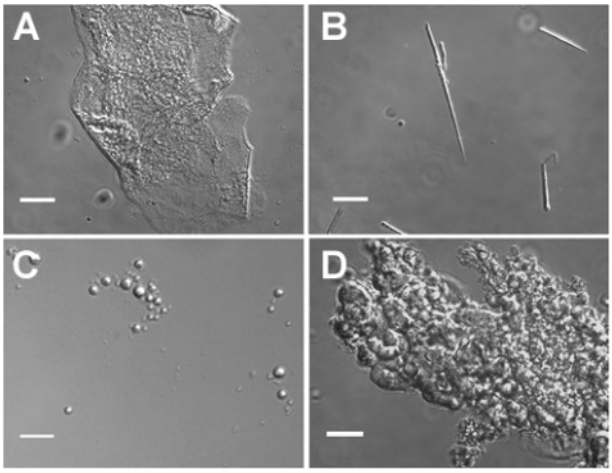

Figure 2. Differential interference contrast (DIC) images of 1% (w/v) aqueous suspensions of K_xL_y block copolypeptides. (A) = $K_{20}L_{20}$ (sheets), (B) = $K_{40}L_{20}$ (fibrils), (C) = $K_{60}L_{20}$ (vesicles), and (D) = $K_{80}L_{20}$ (irregular aggregates). Bars = 5 μm.

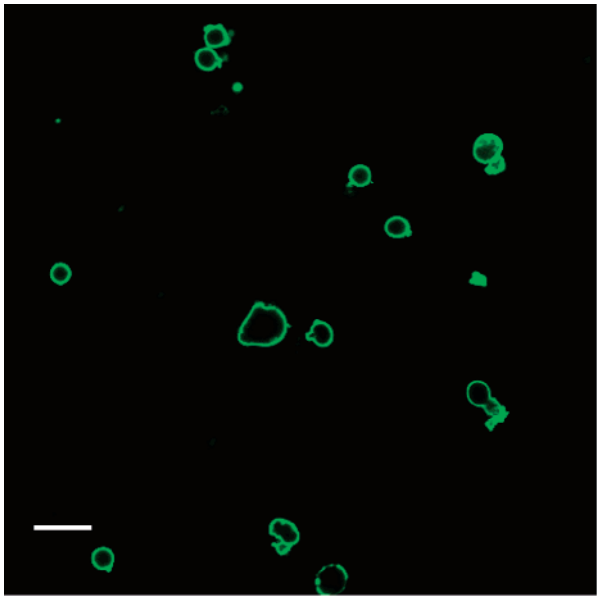

Figure 3. LSCM of a 1% (w/v) $E_{60}L_{20}$ vesicle suspension (Bar = 5 μm).

diameter) were observed by DIC. Further analysis of these vesicles using laser scanning confocal microscopy (LSCM) revealed that the vesicles are unilamellar, since we did not observe any fluorescence intensity within the centers of the vesicles (Figure 3). If the vesicles were multilamellar, or onion-like, we would observe fluorescence intensity throughout the vesicle interior.[17] One could argue that this is not the most accurate method of detecting multiple membranes, especially if there are only a few multilayers, but this possibility is unlikely due to the highly charged nature of the membranes that favors intermembrane repulsion. Also, TEM images (Figure 4) show only unilamellar vesicles, confirming our analysis of the confocal data.[18] Analysis of the $K_{80}L_{20}$ sample showed the presence of a few vesicles, but the bulk of the material was in the form of large disordered aggregates. Since the $K_{60}L_{20}$ sample

(17) (a) Ilhan, F.; Galow, T. H.; Gray, M.; Clavier, G.; Rotello, V. M. *J. Am. Chem. Soc.* **2000**, *122*, 5895−5896. (b) Tsuda, K.; Dol, G. C.; Gensch, T.; Hofkens, J.; Latterini, L.; Weener, J. W.; Meijer, E. W.; De Schryver, F. C. *J. Am. Chem. Soc.* **2000**, *122* 3445−3452.
(18) Materials and methods are available in the Supporting Information.

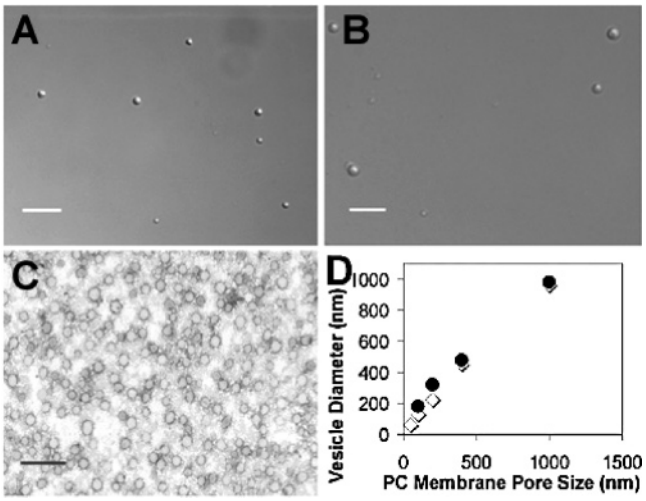

Figure 4. (A and B) DIC images of 1% (w/v) aqueous suspensions of polypeptide vesicles extruded through 1.0 μm PC membranes (Bars = 5 μm). (A) = $K_{60}L_{20}$ and (B) = $E_{60}L_{20}$. (C) Transmission electron microscope (TEM) image of a uranyl acetate negatively stained 0.1% (w/v) $K_{60}L_{20}$ vesicle suspension that was filtered through a 0.1 μm PC membrane before deposition on a Formvar coated copper grid and imaging at 80 keV (Bar = 350 nm). (D) Average diameter of 1% (w/v) aqueous suspensions of $K_{60}L_{20}$ (●) and $E_{60}L_{20}$ (◇) vesicles as a function of extrusion membrane pore size. Vesicle diameters were determined using DLS measured at 90°, and each sample was passed twice through a membrane.

gave vesicles, this length of polylysine was chosen as optimal, and a second series of samples was prepared with oligoleucine lengths varied from 10 to 30 residues with constant K_{60} segments. In these samples, both hydrophobic content and chain conformation were varied since only oligoleucines with greater than ca. 20 residues can adopt stable α-helical conformations.[12] Circular dichroism analysis of (*rac*-K)$_{60}L_y$ samples, where *rac*-K is a statistical 1:1 copolymer of D-lysine and L-lysine and y = 10, 20, or 30, showed that the fraction of α-helical content in the oligoleucine segments increased substantially with domain size: 10% helix for (*rac*-K)$_{60}L_{10}$, 55% helix for (*rac*-K)$_{60}L_{20}$, and 90% helix for (*rac*-K)$_{60}L_{30}$.[18] Upon investigation of the supramolecular assemblies formed by the corresponding L-configuration copolymers, it was found that only the samples with predominantly helical hydrophobes formed vesicles, since $K_{60}L_{10}$ was found to form small micellar aggregates (ca. 25 nm diameter). As a further test of the requirement for helical structure in vesicle formation, we prepared the copolymer K_{60}-(*rac*-L)$_{20}$, where the oligoleucine domain was a statistical 1:1 copolymer of D-leucine and L-leucine that served to disrupt the helical order in this segment.[15] Attempted assembly of this copolymer, which is compositionally identical to $K_{60}L_{20}$, into vesicles failed, yielding only large irregular aggregates. Use of racemic lysine in the hydrophilic component (e.g., (*rac*-K)$_{60}L_{20}$) was found to be less disruptive (Table 1), although some irregular aggregates were observed in addition to vesicles. Finally, vesicle formation was found to be sensitive to overall hydrophobic composition as well, since $K_{60}L_{30}$ formed only a few vesicles with the majority of the material being present as irregular aggregates. Based on these results, the optimized vesicle-forming composition of $K_{60}L_{20}$ was chosen for further evaluation. For comparison, we prepared the anionic copolypeptide counterpart to $K_{60}L_{20}$, namely poly(L-glutamate)$_{60}$-*b*-poly(L-leucine)$_{20}$ or $E_{60}L_{20}$, which was also found to form vesicles (Figure 4B).

The different morphologies observed in the annealed aqueous suspensions of the block copolypeptide samples can be explained. Based upon earlier studies on amphiphilic block copolypeptides, it was known that helical oligoleucine domains prefer to pack side-by-side along their long axes to form relatively flat 2D sheets.[11] The sheetlike morphology is enforced by the presence of the hydrophilic domains, which hinders 3D assembly and gives hydrated, lipidlike membranes. If the lysine-to-leucine ratio is too low, as in $K_{60}L_{30}$, there is not enough polyelectrolyte to sterically stabilize and solubilize the hydrophobic domains, and insoluble aggregates are favored over regular membranes. Similarly, for $K_{20}L_{20}$, only poorly hydrated sheets are formed that are too stiff to curve into spherical vesicles, even over tens of microns. If the lysine-to-leucine ratio is too high, as in $K_{80}L_{20}$, interchain polyelectrolyte repulsions begin to distort the membranes from planarity also resulting in vesicle destabilization. The loss of helicity, as in $K_{60}L_{10}$ and $K_{60}(rac\text{-}L)_{20}$ samples, gives rise to micelles and irregular aggregates since the highly anisotropic packing preference of the helical rods is absent. The spontaneous formation of giant, micron-sized vesicles with $K_{60}L_{20}$ implies that local membrane curvature is low, hinting that the packed rodlike helices yield stiff membranes (Figure 1). Initially, this was surprising since we expected that the membranes of $K_{60}L_{20}$ would be more flexible than those of vesicles formed from uncharged block copolypeptides, e.g., poly(N_ϵ-2-(2-(2-methoxyethoxy)ethoxy)-acetyl-L-lysine)$_{100}$-*b*-poly(L-leucine)$_{20}$, which also have diameters in the micron range.[11] The lack of flexibility in the uncharged copolymers arises since they are rodlike in both domains, allowing hardly any conformational freedom. However, the polylysine segments, although stretched by electrostatic repulsions, should have some configurational freedom and thus some flexibility. Furthermore, the interchain repulsions of the polyelectrolyte segments should destabilize packing of the hydrophobic domains, which could lead to a less ordered, and hence more flexible, hydrophobic membrane core. Conversely, it could be argued that confinement of the polyelectrolyte segments to the membrane interface leads to rigidification of the membrane since electrostatic repulsions lock the polyelectrolyte segments in place. To get a better understanding of the $K_{60}L_{20}$ membrane properties, we evaluated membrane stability under a variety of stimuli including shear/extrusion, osmotic stress, and ionic media.

The $K_{60}L_{20}$ polypeptide vesicles obtained directly from dialysis are polydisperse and range in diameter from ca. 5 μm down to 0.8 μm as determined using DIC and DLS. For applications such as drug delivery via blood circulation, a vesicle diameter of ca. 50 to 100 nm is desired.[19] In previous studies on uncharged polypeptide vesicles, the as-formed micron-sized vesicles could not be reduced in size by liposome-type extrusion techniques and could only be made smaller by more aggressive sonication methods.[11] The inability of the uncharged vesicles to pass through small pore diameter filters was likely due to the rigidity of the membrane, which is composed of wholly rodlike polymer segments. For comparison, uncharged synthetic polymersomes, which are composed of flexible polyethylethylene and poly(ethylene oxide) segments, can be extruded without difficulty.[20] Here, we observed that aqueous suspensions of $K_{60}L_{20}$ vesicles could be extruded through nuclear track-etched polycarbonate membranes with little loss of polypeptide material (<20%). After two passes through a filter, reductions in vesicle diameter to values in close agreement to filter pore size were observed (Figure 4). These results showed that the charged polypeptide vesicles are readily extruded, allowing good control over vesicle diameter in the tens to hundreds of nanometers range. DLS analysis revealed that the extruded vesicles were also less polydisperse than before extrusion and contained no micellar contaminants.[18] The vesicular morphology was also confirmed through TEM imaging of the submicron $K_{60}L_{20}$ suspensions (Figure 4).[18] Thus, it appears that the membranes of the $K_{60}L_{20}$ vesicles are considerably more flexible and compliant than those of purely rodlike uncharged polypeptides. The extruded vesicles were monitored for 6 weeks using DLS and were found to be generally stable since the average diameters did not change for most samples. Only the smallest vesicles (ca. 50 nm diameter) were found to show a gradual increase in size over time (to ca. 60 nm after 6 weeks), possibly due to vesicle fusion. Since the smallest vesicles have the greatest strain due to curvature, it makes sense that these are the least stable. Micron sized $K_{60}L_{20}$ vesicles were found to be very robust, with no visible changes after 3 months at ambient temperature. The vesicles were also found to have high thermal stability. An aqueous suspension of 1 μm vesicles was held at 80 °C for 30 min, after which no vesicle disruption could be detected.[24] Only after heating to 100 °C for 30 min were the vesicles disrupted, yielding large flat membrane sheets.

To test the integrity of the vesicle membranes, we attempted to encapsulate a water soluble cargo. Specifically, Texas Red labeled dextran (3000 Da) was included in the $K_{60}L_{20}$/THF/H_2O mixture during vesicle assembly. The resulting suspension was first dialyzed using a 2000 Da molecular weight cutoff (MWCO) cellulose membrane to prevent loss of dextran during assembly. After exhaustive dialysis against DI water, the vesicle suspension was dialyzed again using a 8000 Da MWCO membrane to remove all nonencapsulated dextran, leaving only the dextran that was encapsulated within the vesicles. The resulting vesicles were found to contain reasonable amounts of encapsulated dextran (Figure 5A),[21] which did not leak out for at least 5 days. As a control, Texas Red-dextran mixed with preformed 1 μm $K_{60}L_{20}$ vesicles, followed by dialysis, was found to be completely absent from the vesicle sample, indicating no adsorption of dextran to the vesicle surface or diffusion into preformed vesicles.[23] Upon extrusion of dextran-containing vesicles, the amount of encapsulated dextran was found to decrease with the number of filter passes, as measured by monitoring fluorescence of the resulting dialyzed vesicle suspensions (Figure 5B). This result indicated that the vesicles must at least partially rupture during the extrusion process, allowing some encapsulated dextran to escape. Using this information, we developed an improved encapsulation protocol, where empty $K_{60}L_{20}$ vesicles were extruded in the presence of the solute to be encapsulated. Using this strategy with Texas Red-dextran, we obtained encapsulation efficiencies after only two filter passes that scaled with dextran concentration and

(19) Kataoka, K.; Kwon, G. S.; Yokoyama, M.; Okano, T.; Sakurai, Y. *J. Controlled Release* **1993**, *24*, 119−132.

(20) (a) Discher, B. M.; Hammer, D. A.; Bates, F. S.; Discher, D. E. *Curr. Opin. Colloid Interface Sci.* **2000**, *5*, 125−145. (b) Discher, D. E.; Eisenberg, A. *Science* **2002**, *297*, 967−973.

(21) Wilhelm, M.; Zhao, C.; Wang, Y.; Xu, R.; Winnik, M. *Macromolecules* **1991**, *24*, 1033−1040.

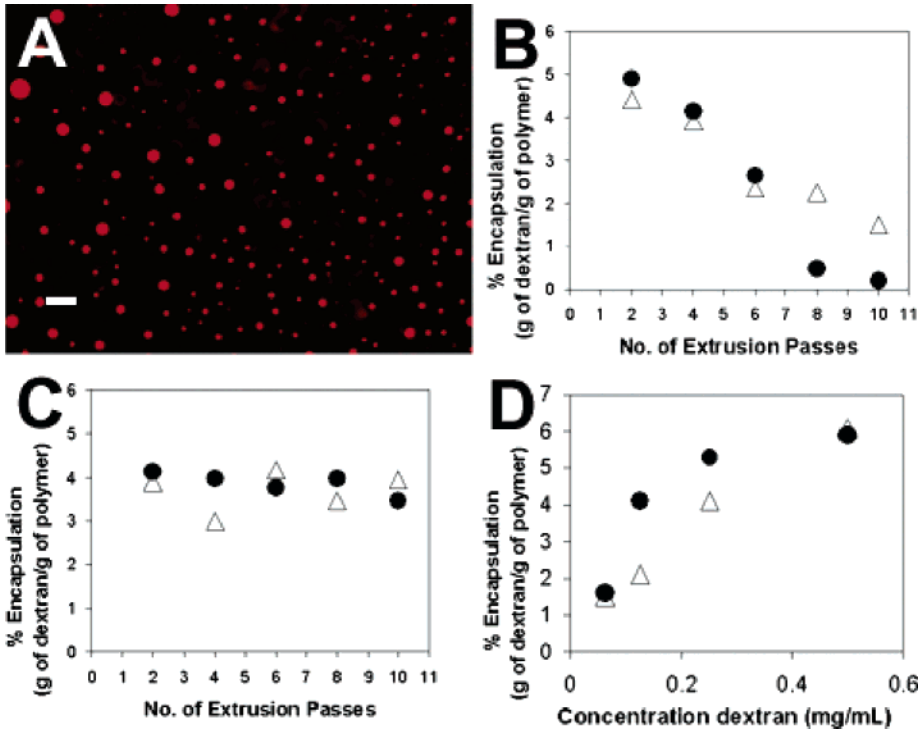

Figure 5. (A) Fluorescence micrograph of a 0.1% (w/v) aqueous suspension of 1.0 μm PC membrane extruded $K_{60}L_{20}$ vesicles formed in the presence of Texas Red labeled dextran (3000 Da) followed by dialysis against DI water (Bar = 5 μm). (B) Dextran remaining in Texas Red-dextran loaded vesicles after multiple extrusions through 0.4 μm PC membranes in DI water. (C) Extrusion of dextran-free vesicles performed in the presence of Texas Red-dextran solution (0.125 mg/mL). (D) Percent encapsulation of Texas Red-dextran after two pass extrusion of dextran-free vesicles through 0.4 μm PC membranes in the presence of different concentrations of Texas Red-dextran solution. (●) $K_{60}L_{20}$. (△) $E_{60}L_{20}$.

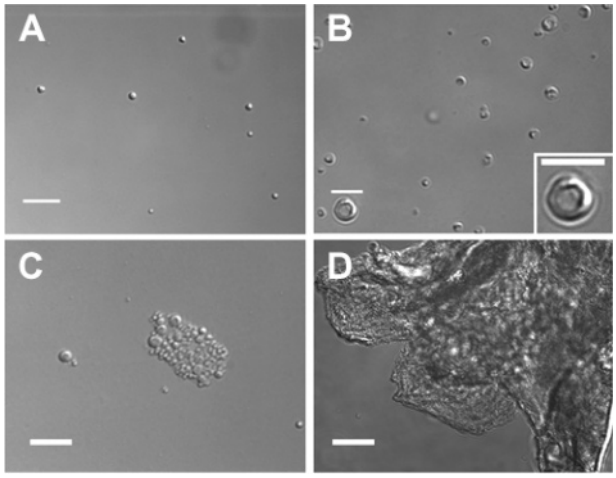

Figure 6. DIC images of 1% (w/v) aqueous suspensions of 1.0 μm PC membrane extruded $K_{60}L_{20}$ vesicles in sodium chloride and sucrose solutions. (A) pure DI water, (B) 0.75 M sucrose (inset shows expanded view of collapsed vesicle), (C) 100 mM NaCl, (D) = 1.0 M NaCl. Bars = 5 μm.

which equalled those seen above (Figure 5C,D). Hence, the processing characteristics of the $K_{60}L_{20}$ vesicles allow one to control vesicle size and encapsulate a solute by a straightforward filtration process.

To examine membrane permeability, $K_{60}L_{20}$ vesicles were subjected to osmotic stress using both uncharged and ionic species. First, saturated sucrose was added to 1 μm vesicles in DI water to give a 250 mM sucrose concentration, after which the vesicles were found by DIC to flatten and wrinkle (Figure 6B), consistent with loss of water from the vesicle interiors in response to the osmotic stress. Dialysis of this suspension restored the vesicles to their original size and shape, indicating that the process is reversible, This result showed that the vesicle membranes are permeable to water, similar to polymersomes and liposomes,[20] but not to the larger sucrose molecules. When 1 μm $K_{60}L_{20}$ vesicles were subjected to sodium chloride solutions, different behaviors were observed. At salt concentrations less than 100 mM, no puckering or flattening of the vesicles was seen, and only some clustering of intact, spherical vesicles was observed (Figure 6C). At salt concentrations greater than 500 mM, vesicle disruption occurred, resulting in formation of large flat membranes (Figure 6D). Since no vesicle flattening was observed, it is possible that the membranes are permeable to salt, which will negate the osmotic stress of the external salt solution. The major effects of salt addition, clumping, and vesicle disruption are most likely tied to the polyelectrolyte chains on the vesicle surfaces. Addition of salt acts to screen intrachain and interchain electrostatic repulsions of the polylysine segments. Since polylysine is a fairly hydrophobic polyelectrolyte, lessening electrostatic repulsions can result in sticky chains that may associate in water, leading to the observed clumping and eventual precipitation as flat sheets at high enough salt concentrations.

Stability of these polypeptide vesicles in ionic media is important for use of these assemblies in applications ranging from personal care products to drug delivery. Although the $K_{60}L_{20}$ vesicles are unstable at high salt concentrations, we found that they are stable in 100 mM PBS buffer as well as serum-free DMEM cell culture media.[18] Addition of serum, which contains anionic proteins, results in vesicle disruption, most likely due to polyion complexation between the serum proteins and the oppositely charged polylysine chains. Accordingly, we

found that the negatively charged polypeptide vesicles prepared using $E_{60}L_{20}$ are stable in DMEM with 10% fetal bovine serum.[18] Based on these results, we believe these charged polypeptide vesicles show potential as enzymatically degradable encapsulants for water soluble solutes as an alternative to liposomes. The advantages of these materials are increased stability, straightforward encapsulation and size control, as well as the potential for facile functionalization of the hydrophilic polypeptide chains at the vesicle surface.

Acknowledgment. The authors thank Lisa Pakstis (University of Delaware) who assisted in the initial evaluation of these materials. This work was supported by a grant from the National Science Foundation (Award No. CTS-0103516).

Supporting Information Available: Details of all materials and measurements. This material is available free of charge via the Internet at http://pubs.acs.org.

JA053557T